6. Design Criteria

6.1 General

The findings of the parametric study, as discussed in Chapter 6, provided a reasonable basis for developing the design criteria for evaluating the hydro-mechanical performance of PWBP in underground coal mines. The study showed that extent of zones having positive volumetric strain (ZoPVS) and seepage rate across the pillar are two critical components for quantifying the hydro-mechanical performance of PWBP.

Based on the outcomes of the parametric study, this chapter describes the development of the design criteria for assessing the mechanical and hydraulic performance of PWBP under varying geo-mining conditions. Statistical regression-based models was developed for predicting the ZoPVS and the seepage rate encompassing the parameters influencing the hydro-mechanical stability of the pillar. A seepage rate severity classification was also proposed based on the field experience in different coal mines and the numerical modelling results. The criteria for the rational design of PWBP was developed considering its long-term hydro-mechanical stability and steady-state controlled seepage rate through the pillar.

6.2 Evaluation of Mechanical Performance

A statistical model was developed using a nonlinear multiple regression analysis for evaluating the mechanical performance in terms of the extent of positive volumetric strain zones (%) in the PWBP in a given geo-mining condition. The results of fifty-three models (Annexure I) were used to establish the relationship using seven independent variables, which included pillar width (m), cover depth (m), mean horizontal stress (MPa), rock mass

compressive strength of coal (MPa), modulus of elasticity of coal and roof/floor (GPa), and the extraction ratio. The nonlinear relationship between the independent and dependent variables was established using the linear relationship of logarithmically transformed data.

The linear regression equation for logarithmically transformed data is of the form shown in Equation 6.1. The equation can be transformed into a power function to formulate the relationship between the dependent and the independent variables, as shown in Equation 6.2.

$$\log_e y = \alpha_0 + \alpha_1 \log_e x_1 + \alpha_2 \log_e x_2 + \alpha_3 \log_e x_3 + \cdots\cdots\cdots + \alpha_n \log_e x_n \quad \ldots(6.1)$$

$$y = k x_1^{\alpha_1} x_2^{\alpha_2} \cdots\cdots x_3^{\alpha_3} \quad \ldots(6.2)$$

Where y is the dependent variable of measuring quantity, k is a constant (e^{α_0}), α_0 is the constant of the linear regression relation, and α_1, α_2, α_3, …, α_n are the coefficients of the independent variables x_1, x_2, x_3, …, x_n, respectively.

The significance of the overall regression analysis was evaluated using the ANOVA output table, the standard error, and the R^2 value. The regression analysis output can be represented as shown in Equation 6.3.

$$F(df_1, df_2) = F, p - value = significance\ F, R^2\ value = adjusted\ R^2\ value \quad \ldots(6.3)$$

The ANOVA table shows the significance of the output of the overall regression analysis. The p-value less than 0.05 confirms a statistically significant regression. The F value shows the ratio of the variance between the sample's mean to the variance within the sample. It is used for testing the null hypothesis. The F value is compared with the F critical value

determined from the F distribution table. If the F value > the F critical value, the null hypothesis is rejected, indicating that the output is statistically significant.

The standard error indicates the average distance between the fitted values and the actual data points. A smaller space suggests a better fit. The R^2 value indicates the extent to which the regression equation can account for the variance of the dependent variable. Its value ranges between 0 to 1, a higher value indicating a better fit.

The empirical relation in Equation 6.4 was established for estimating the ZoPVS in the PWBP.

$$ZoPVS = \frac{2.28\left(\frac{E_i}{E_c}\right)^{0.3} D^{2.39} e^{0.07}}{\sigma_{hi\_c}^{3.88} \sigma_{c\_c}^{0.66} w^{0.82}} \quad \ldots(6.4)$$

Where, ZoPVS = extent of zones having positive volumetric strain, %

E_i = Young's modulus of roof/floor, GPa

E_c = Young's modulus of coal, GPa

D = cover depth, m

e = extraction ratio

σ_{hi_c} = in-situ horizontal stress in coal seam, MPa

σ_{c_c} = rock mass compressive strength of coal, MPa, and

w = pillar width, m

The relation indicates that the ratio of modulus of elasticity of roof/floor and coal i.e. $\left(\frac{E_i}{E_c}\right)$, cover depth (D), and extraction ratio (e) are positively correlated, while the in-situ horizontal stress of coal pillar (σ_{hi_c}), the compressive strength of coal (σ_{c_c}), and pillar width (w) are negatively correlated with the ZoPVS.

Figure 6.1 shows the goodness of fit of the empirical vs. the model estimated ZoPVS. The statistical model can explain 95.1 % variance in ZoPVS. The standard error is only 0.06. The output of the ANOVA table for the overall regression analysis is given in Equation 6.5.

$$F(6,47) = 223.9,\ p - value = 8.34 \times 10^{-32},\ R^2 = 0.951 \quad \ldots(6.5)$$

Similarly, the F value of 223.9 is much greater than the F critical value of 2.1, while the p-value is much less than 0.05, and the R^2 is 0.951, which is closer to 1. Hence, Equation 6.3 can be used to predict the ZoPVS in a pillar with significantly higher accuracy.

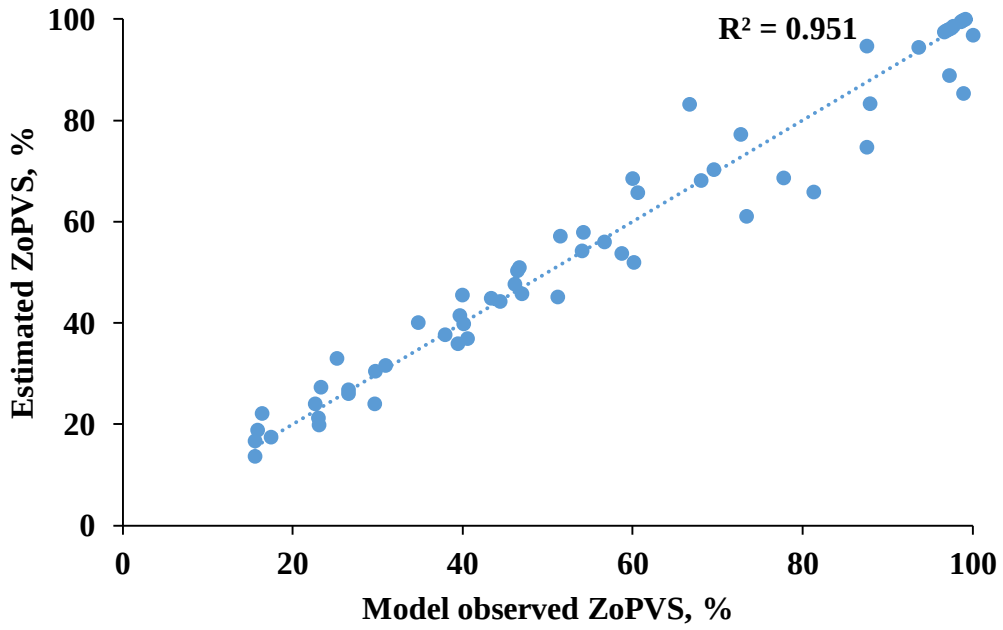

Figure 6.1. Estimated vs. model observed ZoPVS

6.3 Evaluation of Hydraulic Performance

Three thousand five hundred sixty-eight hydro-mechanically coupled models were run to obtain the rate of steady-state water seepage through PWBP in a combination of flow regimes under different geo-mining conditions. A statistical regression analysis similar to Section 6.2 was conducted to establish the relationship between the seepage rate through the barrier pillar and the independently influencing parameters. The independent parameters included cover depth of the working, compressive and tensile strengths for the pillar system, modulus of elasticity of coal, roof, and floor, mean in-situ horizontal stress for the pillar system, pillar width, extraction ratio, and permeability of the rock matrix.

The equations developed for the different flow regimes are described below:

6.3.1 Flow through the Pillar only

This condition considered that water seepage could occur only through pillars as the immediate roof and floor are impermeable. The governing relation for such a flow regime based on the findings of 291 numerical models was obtained as given in Equation 6.6.

$$Q_P = \frac{0.00075 k_P \left(\frac{\sigma_c}{\sigma_T}\right)^{1.11} \left(\frac{E_i}{E_c}\right)^{0.17} D^{0.30} e^{0.01} H^{0.99}}{\sigma_{hi}^{0.38} w^{1.05}} \quad \ldots(6.6)$$

Where, Q_P = seepage rate through the pillar only, 10^{-3} m^3/s/km

w = pillar width, m

e = extraction ratio

σ_{hi} = weighted mean horizontal stress, MPa

σ_c = weighted mean compressive strength of pillar system, MPa

σ_T = weighted mean tensile strength of pillar system, MPa

E_i = Young's modulus of roof/floor, GPa

E_c = Young's modulus of coal, GPa

D = cover depth, m

H = water head, m, and

k_P = permeability of the coal pillar, mD

The relation established through the above equation indicates that the permeability of the coal pillar (k_P), the ratio of modulus of elasticity of roof/floor and coal $\left(\frac{E_i}{E_c}\right)$, the ratio of weighted mean compressive strength to the tensile strength of roof/floor and coal combined $\left(\frac{\sigma_C}{\sigma_T}\right)$, depth of working (D), extraction ratio (e), and water head (H) have a positive correlation, whereas the average in-situ horizontal stress (σ_{hi}), and pillar width (w) negatively correlates with the seepage rate.

The estimates of weighted mean horizontal stress (Equation 6.7), compressive strength (Equation 6.8), and tensile strength (Equation 6.9) were obtained by considering the extent of the zone of influence in the roof and the floor. The modelled zone of influence (MzoI) in the immediate roof and floor was considered up to twice the pillar height.

$$\sigma_{hi} = \frac{(\sigma_{hi\_r}t_r+\sigma_{hi\_p}t_p+\sigma_{hi\_f}t_f)}{(t_r+t_p+t_f)} \quad \ldots(6.7)$$

$$\sigma_c = \frac{(\sigma_{c\_r}t_r+\sigma_{c\_p}t_p+\sigma_{c\_f}t_f)}{(t_r+t_p+t_f)} \quad \ldots(6.8)$$

$$\sigma_T = \frac{(\sigma_{T\_r}t_r+\sigma_{T\_p}t_p+\sigma_{T\_f}t_f)}{(t_r+t_p+t_f)} \quad \ldots(6.9)$$

Where, σ_{hi_r} = mean horizontal stress in the immediate roof, MPa

σ_{hi_p} = mean horizontal stress in the pillar, MPa

σ_{hi_f} = mean horizontal stress in the immediate floor, MPa

σ_{c_r} = mean compressive strength of the immediate roof, MPa

σ_{c_p} = mean compressive strength of pillar, MPa

σ_{c_f} = mean compressive strength of the immediate floor, MPa

σ_{T_r} = mean tensile strength of the immediate roof, MPa

σ_{T_p} = mean tensile strength of pillar, MPa

σ_{T_f} = mean tensile strength of the immediate floor, MPa

t_r = influence zone of the immediate roof, m

t_p = height of the coal pillar, m, and

t_f = influence zone of the immediate floor, m

In the absence of field measure data, the mean horizontal stress in the coal seam and the nether roof and floor were estimated using Equation 3.5 (Sheorey, 1994).

Figure 6.2 shows the goodness of fit of the empirical vs. the model estimated seepage rate through the 'pillar only' conditions. The statistical model can explain 99.6 % variance in seepage rate. The standard error is only 0.09. The output of the ANOVA table for this regression analysis is given in Equation 6.10.

$$F(8, 283) = 32031.6,\ p - value = 0,\ R^2 = 0.996 \quad \ldots(6.10)$$

The F value of 32031.6 is much greater than the F critical value of 1.9, while the p-value is almost zero, and the R^2 value is 0.996, which is closer to 1. Hence, Equation 6.7 can be used to predict the seepage rate with significantly higher accuracy.

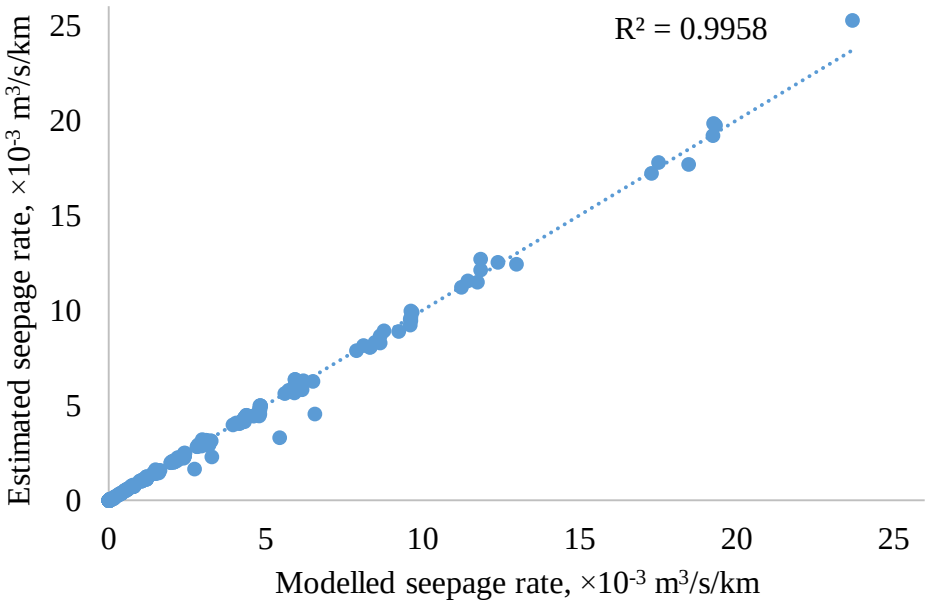

Figure 6.2. Correlation between modelled and estimated seepage rate through the pillar-only

6.3.2 Flow through the Roof only

This condition considered that water seepage could occur only through the immediate roof, and the pillar and the immediate floor are impermeable. The governing relation for such a flow regime was obtained based on the results of 299 numerical models, as shown in Equation 6.11.

$$Q_R = \frac{0.002 k_R \left(\frac{\sigma_c}{\sigma_T}\right)^{0.73} \left(\frac{E_i}{E_c}\right)^{0.11} D^{0.14} e^{0.01} H^{1.03}}{\sigma_{hi}^{0.19} w^{0.92}} \quad \ldots(6.11)$$

Where, Q_R = seepage rate through the floor only, 10^{-3} $m^3/s/km$

w = pillar width, m

e = extraction ratio

σ_{hi} = weighted mean in-situ horizontal stress, MPa (Equation 6.5)

σ_c = weighted mean rock-mass compressive strength, MPa (Equation 6.8)

σ_T = weighted mean rock mass tensile strength, MPa (Equation 6.9)

E_i = Young's modulus of roof/floor, GPa

E_c = Young's modulus of coal, GPa

D = cover depth, m

H = water head, m, and

k_R = permeability of the immediate roof, mD

The relation established through the above equation indicates that the permeability of the roof (k_R), the ratio of modulus of elasticity of roof/floor and coal $\left(\frac{E_i}{E_c}\right)$, the ratio of mean compressive strength to the tensile strength of roof/floor and coal $\left(\frac{\sigma_C}{\sigma_T}\right)$, cover depth (D), extraction ratio (e), and water head (H) have a positive correlation, whereas the average in-situ horizontal stress (σ_{hi}), and pillar width (w) negatively correlates with the seepage rate.

Figure 6.3 shows the fit of the empirical vs. the model estimated seepage rate through the 'roof only' condition. The statistical relation can explain 99.8 % variance in seepage rate. The standard error is only 0.06. The output of the ANOVA table for this regression analysis is given in Equation 6.12.

$$F(8, 291) = 54669.7,\ p - value = 0,\ R^2 = 0.998 \quad \ldots(6.12)$$

The F value of 54669.7 is much greater than the F critical value of 1.9, while the p-value is almost zero, and the R^2 value is 0.998, which is closer to 1. Hence, Equation 6.11 can predict the seepage rate with significantly higher accuracy.

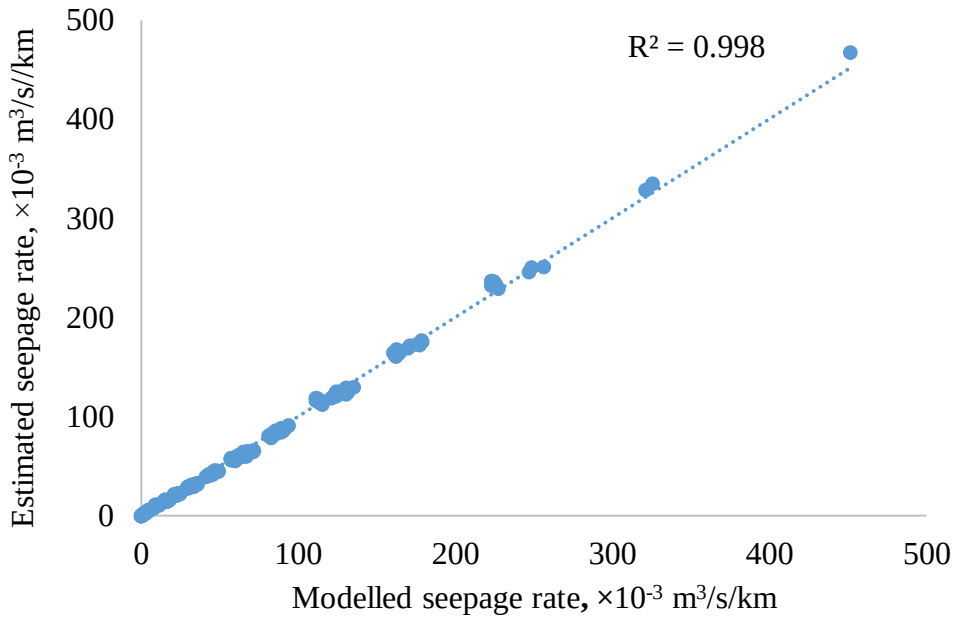

Figure 6.3. Correlation between modelled and estimated seepage rate through the roof-only

6.3.3 Flow through the Floor only

This condition considered that the seepage of water could occur only through the immediate floor as the pillar and immediate roof are impermeable. The governing relation for such a flow regime was obtained using the outcomes of 299 numerical models, as shown in Equation 6.13.

$$Q_F = \frac{0.013 k_F \left(\frac{\sigma_c}{\sigma_T}\right)^{0.03} \left(\frac{E_i}{E_c}\right)^{0.01} D^{0.09} e^{0.02} H^{1.03}}{\sigma_{hi}^{0.15} w^{0.85}} \quad \ldots(6.13)$$

Where, Q_F = seepage rate through the floor only, 10^{-3} m^3/s/km

w = pillar width, m

e = extraction ratio

σ_{hi} = mean horizontal stress, MPa (Equation 6.5)

σ_c = mean rock-mass compressive strength, MPa (Equation 6.8)

σ_T = mean rock mass tensile strength, MPa (Equation 6.9)

E_i = Young's modulus of roof/floor, GPa

E_c = Young's modulus of coal, GPa

D = cover depth, m

H = water head, m, and

k_F = permeability of the immediate floor, mD

The relation established through the above equation indicates that the permeability of the floor (k_F), the ratio of modulus of elasticity of roof/floor and coal $\left(\frac{E_i}{E_c}\right)$, the ratio of the mean compressive strength to the tensile strength of the roof/floor and coal $\left(\frac{\sigma_C}{\sigma_T}\right)$, cover depth (D), extraction ratio (e), and water head (H) have a positive correlation, whereas the average in-situ horizontal stress (σ_{hi}), and pillar width (w) negatively correlates with the seepage rate.

Figure 6.4 shows the fit of the empirical vs. the model estimated seepage rate through the 'floor only' condition. The statistical model can explain 99.9 % variance in seepage rate. The standard error is almost zero. The output of the ANOVA table for overall regression analysis is given in Equation 6.14.

$$F(8, 291) = 1.8 \times 10^7,\ p - value = 0,\ R^2 = 0.999 \quad \ldots(6.14)$$

The F value of 1.8×10^7 is much greater than the F critical value of 1.9, while the p-value is almost zero, and the R^2 value is 0.999, which is closer to 1. Hence, Equation 6.13 can predict the seepage rate with significantly higher accuracy.

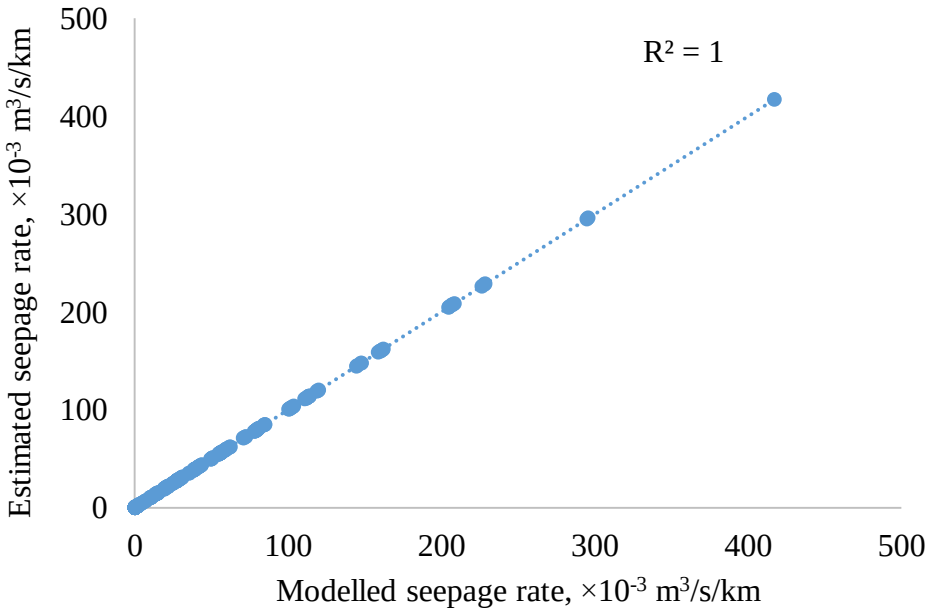

Figure 6.4. Correlation between modeled and estimated seepage rate through the floor-only

6.3.4 Flow through Pillar and Roof

This condition considered that water seepage could occur only through the pillar and immediate roof as the immediate floor is impermeable. Based on the results of 993 numerical models, the governing relation for such a flow regime was obtained as given in Equation 6.15.

$$Q_{PR} = \frac{0.02 k_{PR}^{0.99} \left(\frac{\sigma_c}{\sigma_T}\right)^{0.26} \left(\frac{E_i}{E_c}\right)^{0.03} D^{0.16} e^{0.01H}}{\sigma_{hi}^{0.23} w^{0.93}} \quad \ldots(6.15)$$

Where, Q_{PR} = seepage rate through the pillar and immediate roof, 10^{-3} $m^3/s/km$

w = pillar width, m

e = extraction ratio

σ_{hi} = mean in-situ horizontal stress, MPa (Equation 6.5)

σ_c = mean rock-mass compressive strength, MPa (Equation 6.8)

σ_T = mean rock mass tensile strength, MPa (Equation 6.9)

E_i = Young's modulus of roof/floor, GPa

E_c = Young's modulus of coal, GPa

D = cover depth, m

H = water head, m, and

k_{PR} = weighted average permeability of the pillar and the immediate roof, mD

The weighted average permeability of the pillar and roof combinedly was calculated using Equation 6.16.

$$k_{PR} = \frac{(k_R t_r + k_P t_p)}{(t_r + t_p)} \quad \ldots(6.16)$$

Where, k_R = permeability of the immediate roof, mD

k_P = permeability of the coal pillar, mD

t_r = influence zone of the immediate roof, m, and

t_p = height of the coal pillar, m

The relation established through the above equation indicates that the combined permeability of the pillar and roof (k_{PR}), the ratio of modulus of elasticity of roof/floor and coal $\left(\frac{E_i}{E_c}\right)$, the ratio of mean compressive strength to the tensile strength of roof/floor and coal $\left(\frac{\sigma_C}{\sigma_T}\right)$, cover depth (D), extraction ratio (e), and water head (H) have a positive correlation, whereas the average in-situ horizontal stress (σ_{hi}), and pillar width (w) negatively correlates with the seepage rate.

Figure 6.5 shows the goodness of fit of the empirical vs. the model estimated seepage rate through the 'pillar and roof' condition. The statistical model can explain 99.8 % variance in seepage rate. The standard error is only 0.05. The output of the ANOVA table for this regression analysis is given in Equation 6.17.

$$F(8,885) = 143268,\ p - value = 0,\ R^2 = 0.998 \quad \ldots(6.17)$$

The F value of 143268 is much greater than the F critical value of 1.9, while the p-value is almost zero, and the R^2 value is 0.998, which is closer to 1. Hence, Equation 6.15 can predict the seepage rate with significantly higher accuracy.

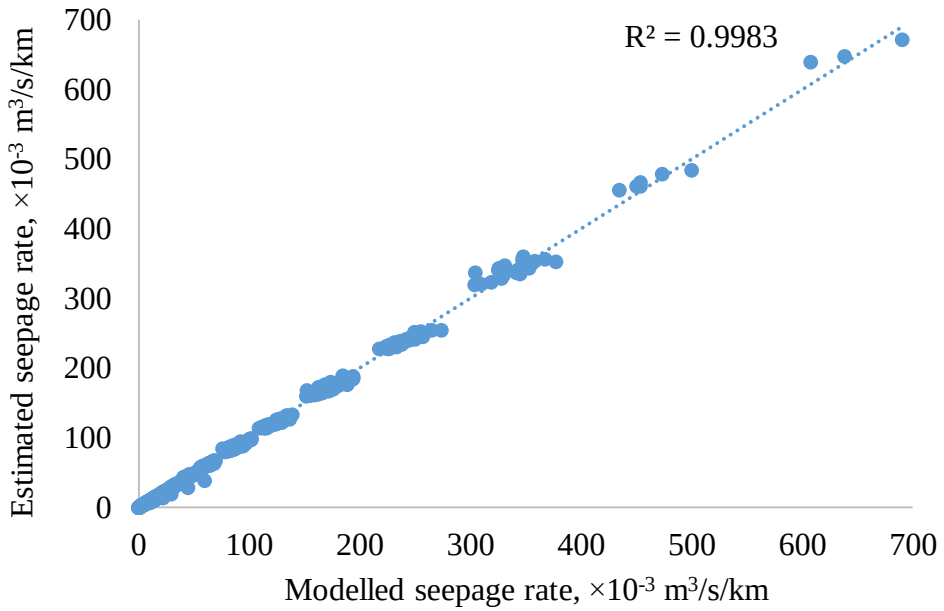

Figure 6.5. Correlation between modelled and estimated seepage rate through pillar and roof

6.3.5 Flow through Pillar and Floor

This condition considered that the seepage of water could occur only through the pillar and immediate floor while the immediate roof is impermeable. The governing relation for such a flow regime was obtained based on the results of 993 numerical models, as given in Equation 6.18.

$$Q_{PF} = \frac{0.007 k_{PF}^{0.98} \left(\frac{\sigma_c}{\sigma_T}\right)^{0.52} \left(\frac{E_i}{E_c}\right)^{0.08} D^{0.23} e^{0.02} H^{1.03}}{\sigma_{hi}^{0.37} w^{0.91}} \quad \ldots(6.18)$$

Where, Q_{PF} = water seepage rate through the pillar and floor, 10^{-3} $m^3/s/km$

w = pillar width, m

e = extraction ratio

σ_{hi} = mean horizontal stress, MPa (Equation 6.5)

σ_c = mean rock-mass compressive strength, MPa (Equation 6.8)

σ_T = mean rock mass tensile strength, MPa (Equation 6.9)

E_i = Young's modulus of roof/floor, GPa

E_c = Young's modulus of coal, GPa

D = cover depth, m

H = water head, m, and

k_{PF} = weighted average permeability of the pillar and immediate floor, mD

The weighted average permeability of the pillar and floor combinedly was calculated using Equation 6.19.

$$k_{PF} = \frac{(k_P t_p + k_F t_f)}{(t_p + t_f)} \quad \ldots(6.19)$$

Where, k_P = permeability of the coal pillar, mD

k_F = permeability of the floor, mD

t_p = height of the coal pillar, m

t_f = influence zone of the immediate floor, m

The relation established through the above equation indicates that the permeability of the pillar and floor (k_{PF}), the ratio of modulus of elasticity of roof/floor and coal $\left(\frac{E_i}{E_c}\right)$, the ratio of the mean compressive strength to the tensile strength of the roof/floor and coal combined $\left(\frac{\sigma_C}{\sigma_T}\right)$, cover depth (D), extraction ratio (e), and water head (H) have a positive correlation, whereas the average in-situ horizontal stress (σ_{hi}), and pillar width (w) negatively correlates with the seepage rate.

Figure 6.6 shows the fit of the empirical vs. the model estimated seepage rate through the 'pillar and floor' condition. The statistical model can explain 99.3 % variance in seepage rate. The standard error is only 0.09. The output of the ANOVA table for this regression analysis is given in Equation 6.20.

$$F(8, 885) = 52367.6,\ p - value = 0,\ R^2 = 0.993 \quad \ldots(6.20)$$

The F value of 52367.6 is much greater than the F critical value of 1.9, while the p-value is almost zero, and the R^2 value is 0.993, which is closer to 1. Hence, Equation 6.18 can predict the seepage rate with significantly higher accuracy.

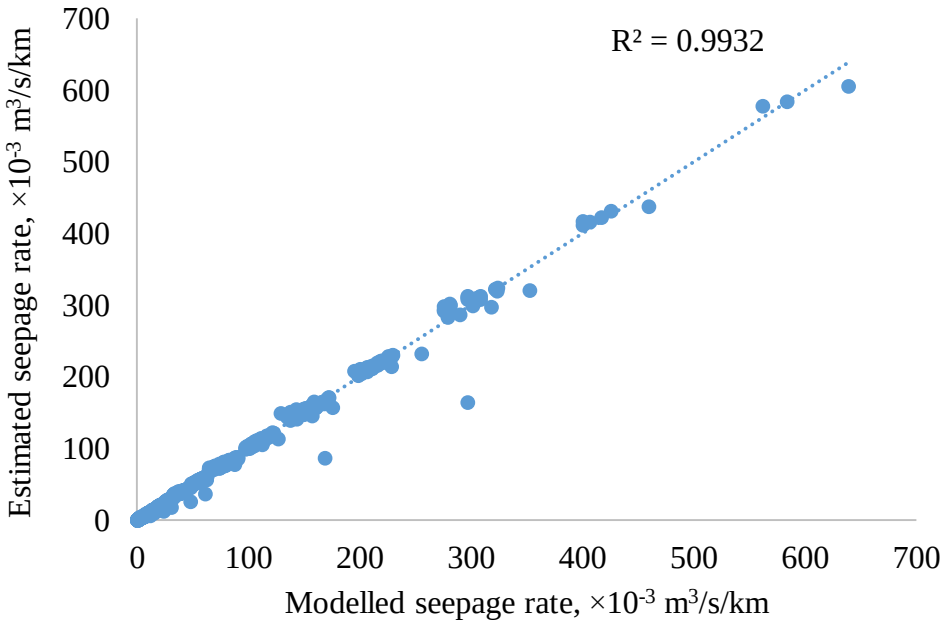

Figure 6.6. Correlation between modelled and estimated seepage rate through pillar and floor

6.3.6 Flow through the Pillar system (Roof, Pillar, and Floor)

This condition considered that water seepage could occur through the pillar, the nether roof, and the floor. The governing relation for such a flow regime was obtained as given in Equation 6.21, based on the results of 893 numerical models.

$$Q_{RPF} = \frac{0.03 k_{RPF} \left(\frac{\sigma_c}{\sigma_T}\right)^{0.21} \left(\frac{E_i}{E_c}\right)^{0.03} D^{0.18} e^{0.02} H^{1.01}}{\sigma_{hi}^{0.26} w^{0.90}} \quad \ldots(6.21)$$

Where, Q_{RPF} = seepage rate through the pillar system, 10^{-3} m^3/s/km

w = pillar width, m

e = extraction ratio

σ_{hi} = mean horizontal stress, MPa (Equation 6.5)

σ_c = mean rock-mass compressive strength, MPa (Equation 6.8)

σ_T = mean rock mass tensile strength, MPa (Equation 6.9)

E_i = Young's modulus of roof/floor, GPa

E_c = Young's modulus of coal, GPa

D = cover depth, m

H = water head, m, and

k_{RPF} = weighted average permeability of the pillar system, mD

The weighted average permeability of the pillar system was calculated using Equation 6.22.

$$k_{RPF} = \frac{(k_R t_r + k_P t_p + k_F t_f)}{(t_r + t_p + t_f)} \quad \ldots(6.22)$$

Where, k_R = permeability of the immediate roof, mD

k_P = permeability of the coal pillar, mD

k_F = permeability of the immediate floor, mD

t_r = influence zone of the immediate roof, m

t_p = height of the coal pillar, m, and

t_f = influence zone of the immediate floor, m

The relation established through the above equation indicates that the permeability of the roof, pillar, and floor (k_{RPF}), the ratio of modulus of elasticity of roof/floor and coal $\left(\frac{E_i}{E_c}\right)$, the ratio of the mean compressive strength to the tensile strength of the roof/floor and coal combined $\left(\frac{\sigma_C}{\sigma_T}\right)$, cover depth (D), extraction ratio (e), and water head (H) have a positive correlation, whereas the average in-situ horizontal stress (σ_{hi}), and pillar width (w) negatively correlates with the seepage rate.

Figure 6.7 shows the goodness of fit of the empirical vs. the model estimated seepage rate through the 'pillar system'. The statistical model can explain 99.9 % variance in seepage rate. The standard error is only 0.06. The output of the ANOVA table for this regression analysis is given in Equation 6.23.

$$F(8, 885) = 137124,\ p - value = 0,\ R^2 = 0.999 \quad \ldots(6.23)$$

The F value of 137124 is much greater than the F critical value of 1.9, while the p-value is almost zero, and the R^2 value is 0.999, which is closer to 1. Hence, Equation 6.21 can predict the seepage rate with significantly higher accuracy.

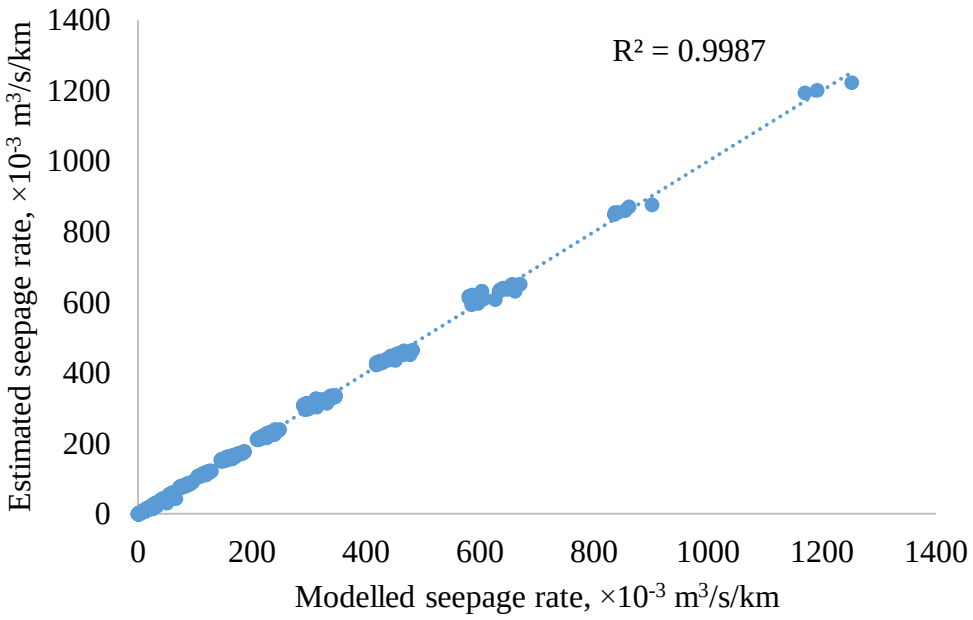

Figure 6.7. Correlation between modelled and estimated seepage rate through pillar system

6.4 Seepage Rate Severity Classification

The modelling-based assessment of water seepage rate for different flow regimes showed that the maximum seepage rate among the various possible combinations was observed through the pillar system. The same was also confirmed during field investigations in several mines. Hence, the subsequent analysis in this study considered the worst seepage rate through the pillar system.

Accordingly, a classification system was proposed to assess the expected severity of water seepage rate across the PWBP (Table 6.1) based on the data compiled in terms of the rate of pumping, the makeup of the water during monsoon and post-monsoon, and the standby time of the pumping operation in the coal mines. It considers the minimum seepage rate that will create knee-depth ponding (water accumulation of 0.5 m height from the floor) up to two pillar distances from the row of PWBP in less than one day, 1-3 days, and more than three

days. The width and height of development galleries have been considered as 5 m, and 3 m, respectively, and the pillar size has been referred from Regulation 111 of CMR 2017 (DGMS 2017) for this purpose. The estimated reservoir capacity for knee-depth ponding up to two pillars is about 1.2×10^4 m^3/km (3.1×10^6 gallons/km) of pillar length.

Coal mines plan to dewater the makeup of mine water daily to maintain the water level in the main sump as their standard practice. The average standby time of pumping operation varies from 10-12 hours daily. The seepage rate of 315×10^{-3} m^3/s/km (5000 GPM/km) is estimated to fill up the given reservoir within the standby time of 10 hours. This seepage rate of 315×10^{-3} m^3/s/km (5000 GPM/km) has been reckoned as the maximum allowable seepage rate for a practically manageable controlled buildup of water in the mine.

Table 6.1. Classification of the Severity of water seepage rate in Indian Coal Mines

Class	Severity	Time (days)	Seepage rate, $10^{-3}m^3$/s/km (GPM/km)	Remarks
I	Low	>3	<95 (1500)	It can be managed easily without any strain on the normal productivity of the mine
II	Moderate	1-3	95-315 (1500-5000)	It is moderately challenging to manage such seepage rate as it may affect the normal production of the mine
III	High	<1	> 315 (5000)	Extremely difficult to manage such seepage rate, which has a considerable adverse effect on mine productivity

6.5 Adequacy of Barrier Pillar Width

Table 6.2 shows the variation in ZoPVS (columns 3,7) and the seepage rate (columns 4,8) across the pillars of progressively reducing width (columns 2,6), subjected to a water head of 100 % under the cover depth of 100, 250, and 350 m for hard and soft rock conditions. The pillar width has been reduced in steps of 5 m, starting with 50 m for a cover depth of 100

m and 100 m for cover depths of 250m and 350m to evaluate the resultant variation in ZoPVS and the total seepage rate through the pillar till the ZoPVS of 100 % was achieved for the given set of conditions. Columns 5 and 9 of the table depict the rate of change in seepage rate through pillars of two consecutive widths in the table. These estimates are based on the weighted permeability of 820 mD for the pillar system. The ZoPVS was calculated as the % of the number of zones having positive volumetric strain with respect to the total number of zones in the barrier pillar.

Table 6.2. ZoPVS and seepage rate across PWBP subjected to water head of 100 % of cover depth

Strength condition	**Hard**				**Soft**			
Depth, m	Width, m (x_i)	ZoPVS, %	Seepage rate, 10^{-3} m^3/s/km (y_i)	Rate of change in seepage rate $\left(\frac{y_i - y_{i-1}}{x_{i-1} - x_i}\right)$	Width, m ($\dot{x_\iota}$)	ZoPVS, %	Seepage rate, 10^{-3} m^3/s/km ($\dot{y_\iota}$)	Rate of change in seepage rate $\left(\frac{\dot{y_\iota} - \dot{y_{\iota-1}}}{\dot{x_{\iota-1}} - \dot{x_\iota}}\right)$
(1)	(2)	(3)	(4)	(5)	(6)	(7)	(8)	(9)
100	50.0	22.1	209.7		50.0	29.8	211.5	
	45.0	24.2	231.1	4.3	45.0	32.7	233.1	4.3
	40.0	26.9	257.5	5.3	40.0	36.3	259.7	5.3
	35.0	30.2	290.9	6.7	35.0	40.7	293.4	6.7
	30.0	34.6	335.2	8.9	30.0	46.7	338.1	8.9
	25.0	40.6	396.1	12.2	25.0	54.8	399.5	12.3
	20.0	49.3	485.6	17.9	20.0	66.5	489.9	18.1
	15.0	63.3	631.7	29.2	15.0	85.3	637.2	29.5
	10.0	89.8	914.3	56.5	10.0	100.0	922.2	57.0
	5.0	100.0	1716.1	160.4				
250	100.0	26.3	291.5		100.0	35.4	294.0	
	95.0	27.6	305.9	2.9	95.0	37.2	308.6	2.9
	90.0	28.8	321.1	3.1	90.0	38.9	323.9	3.1
	85.0	30.4	338.7	3.5	85.0	41.0	341.7	3.6
	80.0	32.0	357.7	3.8	80.0	43.1	360.9	3.8
	75.0	33.9	379.8	4.4	75.0	45.7	383.1	4.4
	70.0	36.1	404.8	5.0	70.0	48.7	408.3	5.0
	65.0	38.5	433.3	5.7	65.0	52.0	437.1	5.8
	60.0	41.4	466.3	6.6	60.0	55.8	470.4	6.7

	55.0	44.6	505.0	7.7	55.0	60.2	509.4	7.8
	50.0	48.5	550.9	9.2	50.0	65.3	555.7	9.3
	45.0	53.2	607.0	11.2	45.0	71.8	612.3	11.3
	40.0	59.1	676.3	13.8	40.0	79.6	682.1	14.0
	35.0	66.3	764.0	17.5	35.0	89.4	770.6	17.7
	30.0	76.1	880.5	23.3	30.0	100.0	888.2	23.5
	25.0	89.2	1040.4	32.0				
	20.0	100.0	1275.6	47.0				
	100.0	28.7	410.2		100.0	38.7	413.7	
	95.0	30.2	430.4	4.1	95.0	40.7	434.2	4.1
	90.0	31.5	451.9	4.3	90.0	42.5	455.8	4.3
	85.0	33.3	476.7	5.0	85.0	44.9	480.8	5.0
	80.0	35.0	503.4	5.3	80.0	47.1	507.8	5.4
	75.0	37.1	534.4	6.2	75.0	50.0	539.1	6.3
	70.0	39.5	569.6	7.0	70.0	53.2	574.5	7.1
	65.0	42.1	609.8	8.0	65.0	56.8	615.1	8.1
350	60.0	45.2	656.2	9.3	60.0	61.0	661.9	9.4
	55.0	48.8	710.6	10.9	55.0	65.8	716.8	11.0
	50.0	53.0	775.2	12.9	50.0	71.4	781.9	13.0
	45.0	58.2	854.2	15.8	45.0	78.5	861.6	15.9
	40.0	64.6	951.6	19.5	40.0	87.1	959.9	19.7
	35.0	72.5	1075.1	24.7	35.0	97.8	1084.4	24.9
	30.0	83.2	1239.0	32.8	30.0	100.0	1249.8	33.1
	25.0	97.6	1464.0	45.0				
	20.0	100.0	1795.0	66.2				

The study shows that at 100m depth, ZoPVS for the 50 m wide pillar was only 22 %, while the seepage rate through the pillar was about 209.7×10^{-3} $m^3/s/km$ (3330 GPM/km). The pillar achieved 100 % of ZoPVS as its width was reduced to 8.8 m. The rate of change in seepage through the pillar increased from 4.3×10^{-3} $m^3/s/km$ (67.9 GPM/km) to 160.4×10^{-3} $m^3/s/km$ (2545.5 GPM/km) per m of pillar width for a reduction in pillar width from 50 m to 5 m. A similar study for soft strata condition shows that 100 % of ZoPVS was achieved for a pillar width of 12.4 m. The rate of change in seepage through the pillar increased from 4.3×10^{-3} $m^3/s/km$ (68.4 GPM/km) to 57×10^{-3} $m^3/s/km$ (905 GPM/km) per m of pillar width for a reduction in pillar width from 50 m to 10 m.

As the cover depth increased to 250 m, the pillar of 100 m width produced ZoPVS of 26.3 % under hard rock conditions and 35.4 % in soft rock conditions. The seepage rate through these pillars was 291 $\times 10^{-3}$ m^3/s/km (4626.6 GPM/km) and 294 $\times 10^{-3}$ m^3/s/km (4667 GPM/km) in the hard and soft strata conditions respectively. The ZoPVS of 100 % of attained by 21.9 m wide pillar in hard strata condition and 30.8 m pillar in soft strata condition. Similarly, at the cover depth of 350 m, a pillar of 100 m width produced ZoPVS of 28.7 % under hard rock conditions and 38.7 % in soft rock conditions. The seepage rate through these pillars was 410.2 $\times 10^{-3}$ m^3/s/km (6510) and 413.7 $\times 10^{-3}$ m^3/s/km (6567 GPM/km) in the hard and soft strata conditions. The ZoPVS of 100 % was attained for a pillar width of 24.2 m in hard and 34 m in soft strata conditions in this condition.

The most significant jump in the rate of change in seepage was noted as the pillars achieved 100 % of ZoPVS, marking the onset of their unstable hydraulic behaviour in all the above conditions. The exponentially increased rate of water seepage at this stage signifies its piping failure, which may cause inadvertent inundation in the mine. Accordingly, the maximum pillar width for ZoPVS of 100 % has been considered as the critical width in this dissertation. The study of induced vertical stress in the pillar at this stage at cover depths of 250 and 350 m also confirmed its relaxation, marking the onset of their mechanical instability as noted in some of the previous studies (Cook et al., 1971; Wagner,1974; Morsy, 2003). However, similar behaviour at 100 m depth could be confirmed only for the much lower widths of 3 and 7 m in the hard and soft strata conditions, respectively.

Table 6.3 shows the model estimated rate of water seepage through the 60 m wide barrier pillar as mandated under the existing provisions of the CMR'2017 (DGMS 2017) vis-à-vis the critical pillar width subjected to water head of 25–100% of the cover depth of 100–350

m in soft and hard strata conditions. The study indicated that the size of PWBP need not be the same for the avoidance of its piping failure, irrespective of the cover depth. The analysis of the result shows that for the pillar width of 60 m, the seepage rate remains almost the same for the low-high strength of the rock. A pillar width of 8.8–12.4 m was the critical pillar size for its piping failure at the shallow cover depth of 100 m, while a pillar width of 21.9–30.8 m was critical at a moderate depth of 250 m and 24.2–34 m at the high cover depth of 350 m for this condition in the hard and the soft rock conditions.

Table 6.3. Analysis of Seepage Rate Characteristics of Pillar System

Depth, m	Condition	Pillar Width, m		Seepage Rate for Head in % of depth, 10^{-3} m^3/s/km							
				25		50		75		100	
		Hard	Soft	Hard	Soft	Hard	Soft	Hard	Soft	Hard	Soft
100	CMR'17	60	60	49	49	98	99	147	149	197	199
	Critical	8.8	12.4	253	187	510	376	768	567	1027	758
250	CMR'17	60	60	128	129	257	259	387	390	517	522
	Critical	21.9	30.8	289	214	583	430	878	648	1174	867
350	CMR'17	60	60	179	181	361	364	544	549	728	734
	Critical	24.2	34	372	275	749	553	1127	1095	1507	1114

The study of water seepage rate through the CMR recommended width of 60 m for different cover depths and variable water head showed its reducing trend with a reduction in water head at a given cover depth. The seepage rate reduced from 199 to 49 $\times 10^{-3}$ m^3/s/km (3152 to 778 GPM/km) in the soft rock condition and 197 to 49 $\times 10^{-3}$ m^3/s/km (3125 to 771 GPM/km) in the hard rock condition at the cover depth of 100 m. At the increased cover depth of 250m, the seepage rate reduced from 517 to 128 $\times 10^{-3}$ m^3/s/km (8207 to 2024 GPM/km) in the hard and 522 to 129 $\times 10^{-3}$ m^3/s/km (8279 to 2042 GPM/km) in the soft rock condition. It reduced from 728 to 179 $\times 10^{-3}$ m^3/s/km (11548 to 2848 GPM/km) in the

hard and 734 to 181 $\times 10^{-3}$ m^3/s/km (11650 to 2873 GPM/km) in the soft rock condition for a similar reduction in water head at the cover depth of 350 m. The decreasing trend of water seepage rate is confirmed even for the critical pillar widths. This proves that proactive control of the maximum water head can help control the seepage rate through a barrier pillar in the mine.

The seepage rate produced by the 60 m wide pillar is about 37 % less than the maximum permissible seepage rate for the worst condition of water head at 100 m cover depth. On the other hand, the water seepage rate through such pillar is above the permissible seepage rate limit for water head of 75 % and above at 250 m cover depth and 50 % and above at 350 m cover depth. These observations indicate that the prevailing guideline for the adoption of 60 m wide pillar is resulting in avoidable loss of coal at shallow depth without any compromise in the efficacy of the barrier. On the contrary, it is unable to contain the water seepage rate causing additional pumping strain in deep mine workings in the absence of any guideline for a proactive head control to keep the seepage rate under control.

Table 6.4 shows the desired width of the PWBP for a controlled water seepage rate (maximum allowable seepage rate of 315 $\times 10^{-3}$ m^3/s/km (5000 GPM/km)) in soft and hard rock conditions when subjected to a water head of 25–100 % at the cover depth varying from 100–350 m. The observations indicate that the PWBP width needs to be increased with the increasing head for a controlled seepage rate. The required width of PWBP varies from 2.6-5.5 times the critical width for the worst possible water head for this range of cover depth. It is observed that the pillar size for the maximum allowable seepage rate does not vary significantly with rock strength. However, the critical width is significantly affected by the strength of the rock. The critical width of the pillar is 8.8 and 12.4 m for hard and soft rock

conditions at 100 m depth, and it increases to 24.2 and 34 m at 350 m depth. Hence, the ratio of pillar width for the maximum allowable seepage rate to the critical width is higher for hard rock as compared to the soft rock condition. A pillar width of 32.4 m is sufficient for containing the flow within the allowable limit at 100 m cover depth, but it significantly increases to 92.8-134.6 m at the higher cover depth of 250-350 m. However, the required pillar width was reduced to 43-63 m for the regulated water head of 50% of cover depth in these conditions.

Table 6.4. Desired width for controlled flow through the pillar system

Depth, m	Width for piping failure, m		Desired width for water head in % of depth, m							
			25		**50**		**75**		100	
	Hard	Soft	Hard	Soft	Hard	Soft	Hard	Soft	Hard	Soft
100	8.8	12.4	8.8	12.4	14.9	15	23.3	23.5	32	32.4
250	21.9	30.8	21.9	30.8	42.9	43.3	66.9	67.6	91.9	92.8
350	24.2	34	29	34	62.2	62.8	97.3	98	133.3	134.6

6.6 Development of Design Criteria

Figures 6.8(a)–6.10(b) show the combined plot of ZoPVS and the corresponding water seepage rate for the varying pillar width in the hard and soft rock conditions when subjected to a water head of 25-100 % at the cover depth of 100, 250, and 350 m. These plots consistently confirm the characteristic value of ZoPVS for critical pillar width corresponding to the piping failure and the desired pillar widths for the controlled seepage rate. Table 6.5 compiles the critical and the desired pillar widths for controlled seepage rate at different cover depths for the soft and hard rock conditions.

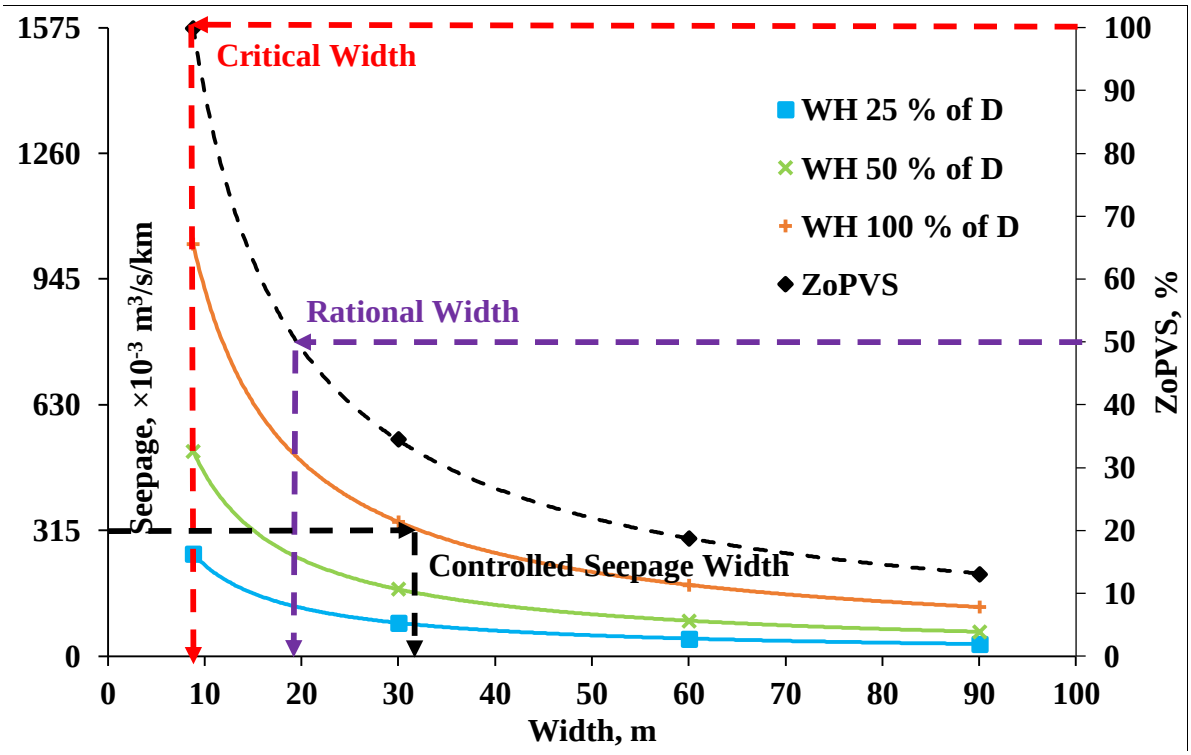

Figure 6.8(a). Seepage rate and ZoPVS for varying pillar width in hard rock conditions at a cover depth of 100 m for different water heads (WH)

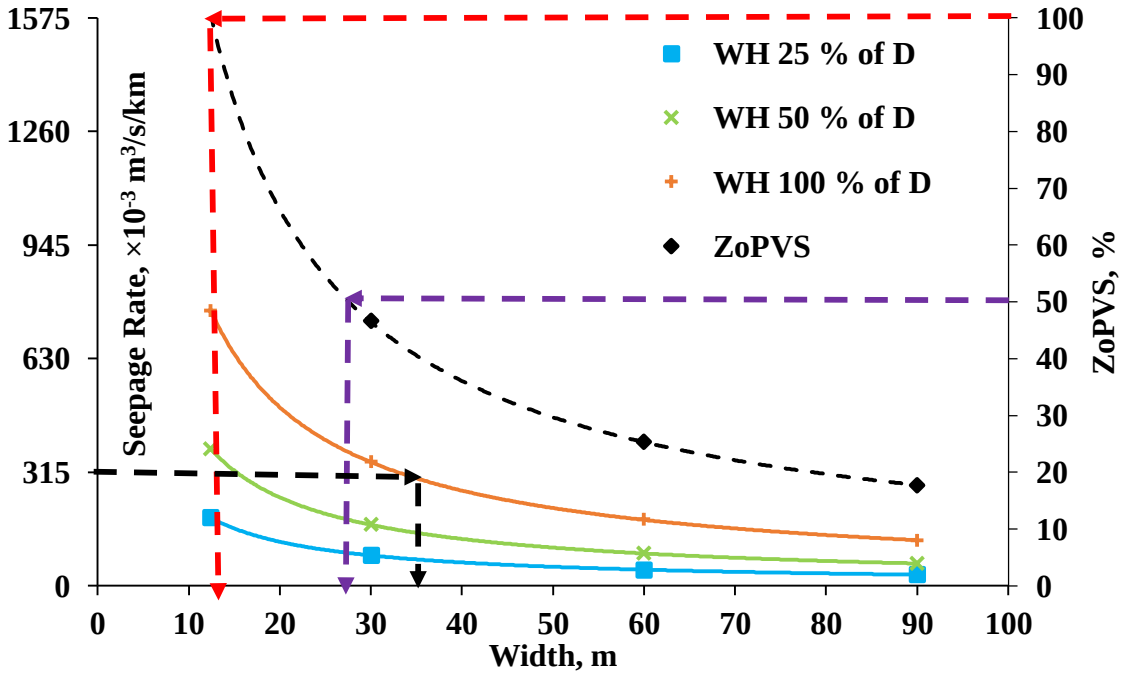

Figure 6.8(b). Seepage rate and ZoPVS for varying pillar width in soft rock conditions at a cover depth of 100 m for different water heads (WH)

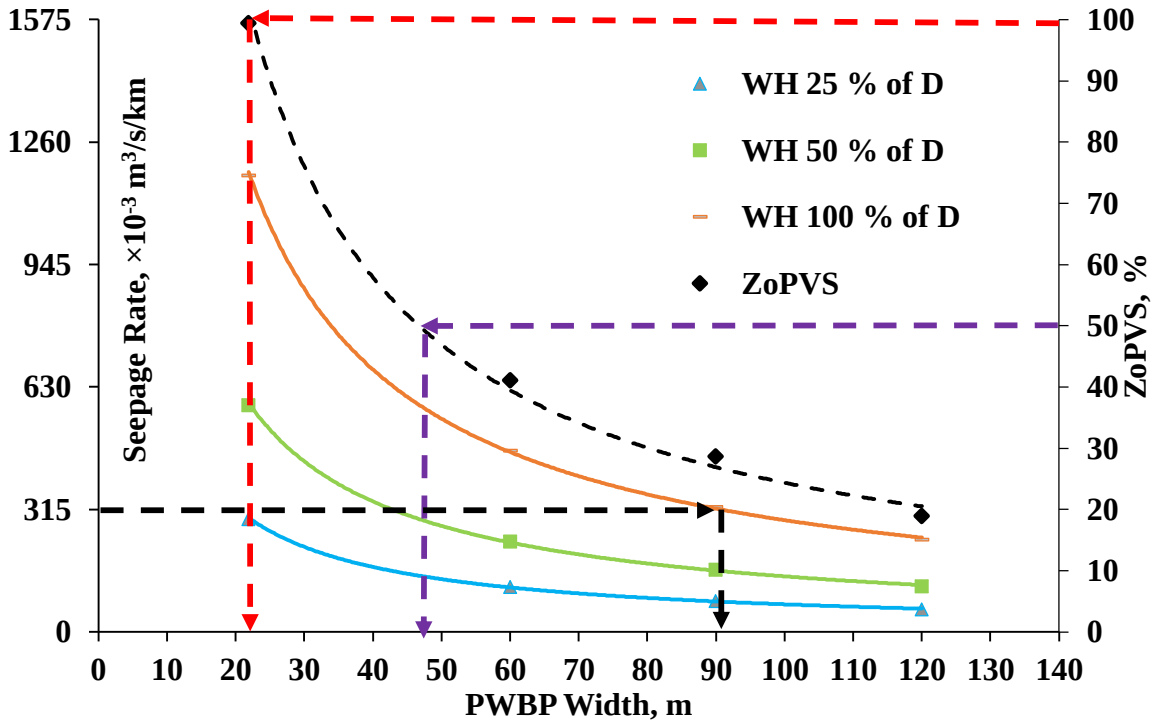

Figure 6.9(a). Seepage rate and ZoPVS for varying pillar width in hard rock conditions at a cover depth of 250 m for different water heads (WH)

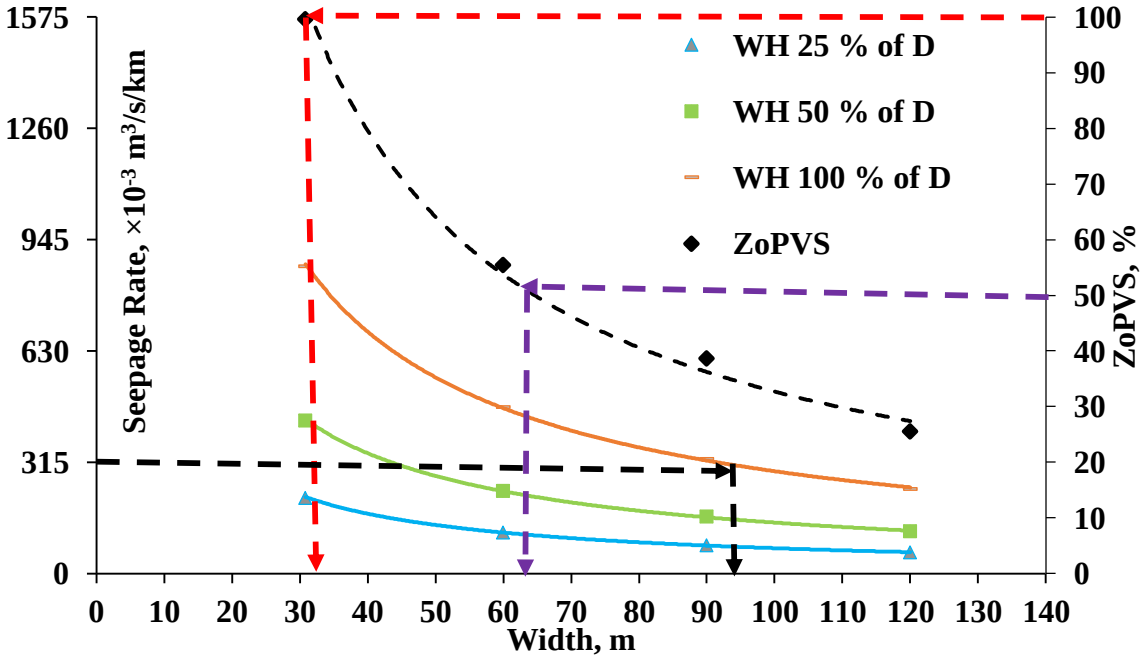

Figure 6.9(b). Seepage rate and ZoPVS for varying pillar width in soft rock conditions at a cover depth of 250 m for different water heads (WH)

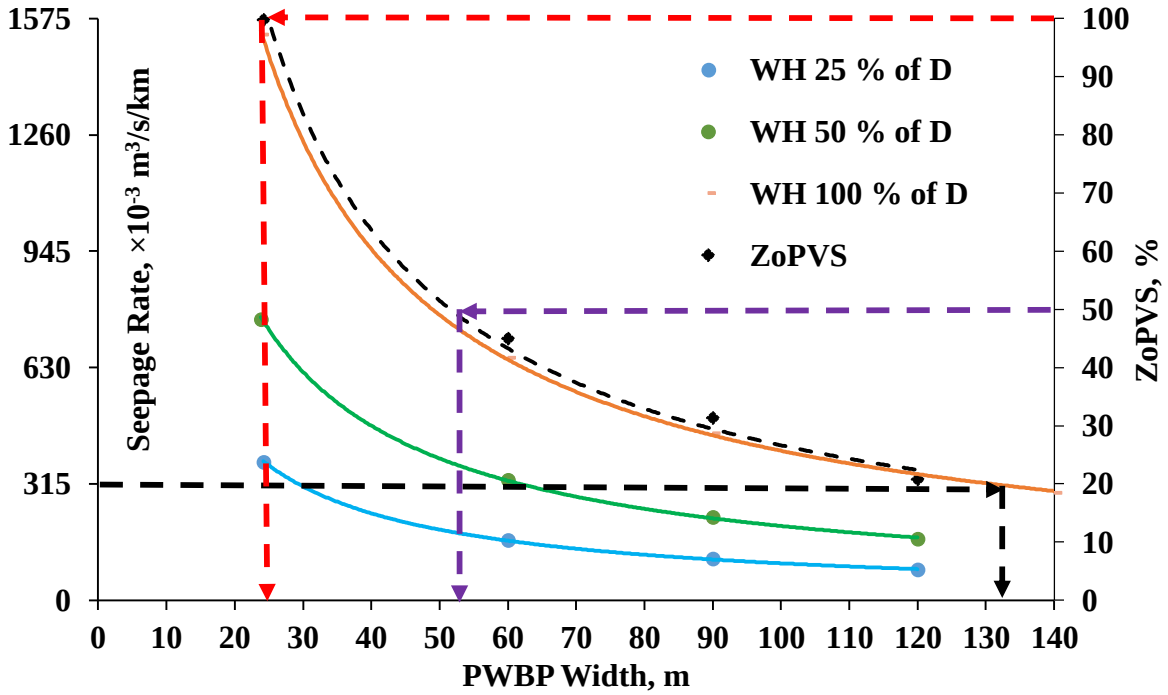

Figure 6.10(a). Seepage rate and ZoPVS for varying pillar width in hard rock conditions at a cover depth of 350 m for different water heads (WH)

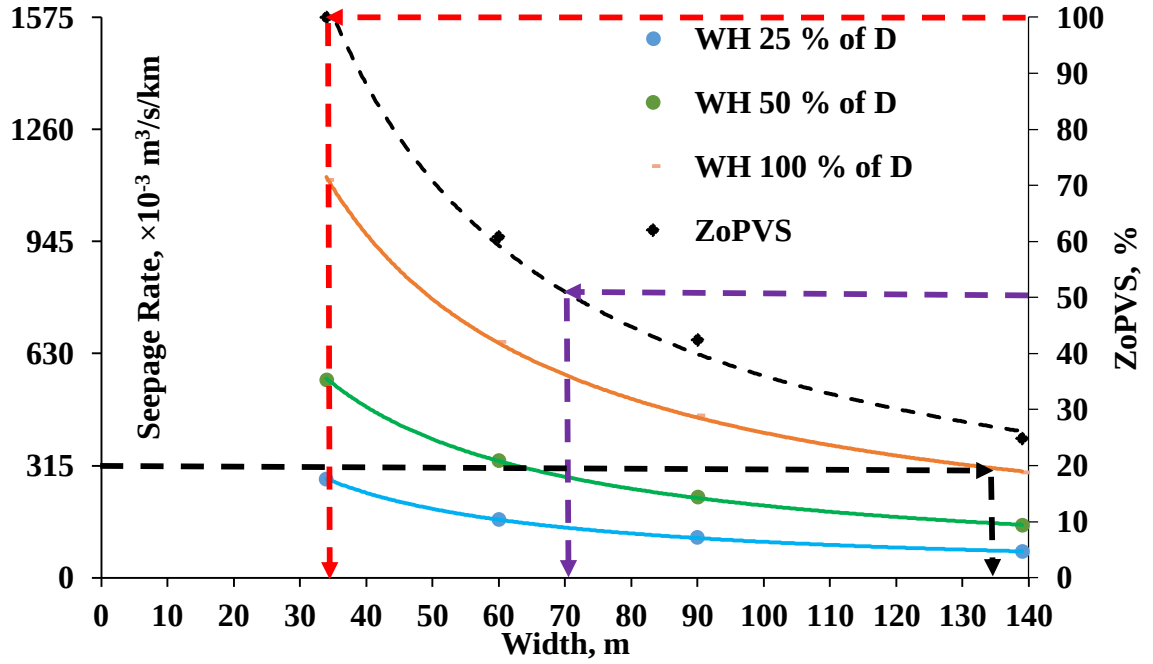

Figure 6.10(b). Seepage rate and ZoPVS for varying pillar width in soft rock conditions at a cover depth of 350 m for different water heads (WH)

Column (2) of Table 6.5 shows the critical width of the pillar for hard and soft rock conditions at the cover depth of 100-350 m, as shown in column (1). Column (3) depicts the pillar width required for containing the seepage rate to the maximum allowable limit of 315×10^{-3} $m^3/s/km$ (5000 GPM/km) for keeping the seepage rate under control, considering the knee-depth ponding criteria. The overall objective is to design a PWBP which can not only provide safety against the danger of inadvertent inundation due to failure of the pillar but also contribute to effective control of water seepage rate. Accordingly, the rational width of PWBP is decided, corresponding to 50 % of ZoPVS for the critical width. Column (4) compiles the corresponding values of the rational pillar width at different cover depths for the hard and soft rock conditions. The plots, as depicted in Figure 6.8(a)-6.10(b), consistently confirm a controlled seepage rate of water along with the physical stability of the pillar (being ensured at 50 % of the critical ZoPVS value for piping failure) for its long term acceptable performance.

The estimated rational width varies from 19.6-53.4 m for the hard rock conditions and 27.7-75 m for soft rock conditions at the cover depth of 100-350 m. The desired water head for controlled seepage rate through these rational pillar widths varies from 64-152.4 m for hard rock and 86.8-205.7 m for soft rock conditions.

Table 6.5. Estimates of rational pillar widths and desired water head at different cover depths

Depth, m (1)	Critical width, m (2)		**Desired pillar width, m (3)**		Rational pillar width, m (4)		Desired water head, m (5)	
	Hard (a)	Soft (b)	**Hard (a)**	**Soft (b)**	Hard (a)	Soft (b)	Hard (a)	Soft (b)
100	8.8	12.4	**32**	**32.4**	19.6	27.7	64	86.8
150	14.7	20.8	**51.5**	**52**	32.7	46	99.3	134.2
200	19.1	26.9	**71.6**	**72.3**	42.2	59.2	123.8	166.9
250	21.9	30.8	**91.9**	**92.8**	48.4	67.8	139.5	188
300	23.5	33.1	**112.4**	**113.5**	51.9	72.5	148.4	199.5
350	24.2	34	**133.3**	**134.6**	53.4	75	152.4	205.7

6.7 Suggested Approach for the Rational Design of PWBP

Based on the findings of the study, as illustrated above, a generalised procedure for estimating the rational size of PWBP can be prepared in the form of a flow chart (Figure 6.11). The approach requires site-specific data on cover depth, extraction ratio, worst expected water head, H_w along with pertinent geo-mechanical properties of the coal seam and the immediate roof in terms of the modulus ratio of immediate roof/floor and coal pillar, the compressive strength of the coal, the ratio of the mean compressive strength and tensile strength of the pillar system as contained in Equation 6.4 for estimating the ZoPVS for a given width of the pillar and corresponding rate of seepage through pillar system using Equation 6.21.

Step 1: The characteristic curves of ZoPVS and seepage rate are obtained for changing widths of the barrier pillar.

Step 2: The critical width of the pillar, w_c corresponding to ZoPVS of 100 %, the controlled seepage rate width, w_{5000} corresponding to the seepage rate of 315×10^{-3} $m^3/s/km$ (5000 GPM/km) and the rational pillar width corresponding to ZoPVS of 50 % are marked on the plot.

Step 3: The water head corresponding to the seepage rate of 315×10^{-3} $m^3/s/km$ (5000 GPM/km) is estimated for the rational width of the pillar. This is marked as the water head for the controlled seepage rate, H_R through the rational pillar width.

Step 4 : The difference between the H_w and the H_R is obtained for planned proactive drainage of the reservoir to maintain the prevailing water head on the reservoir side not exceeding the H_R value.

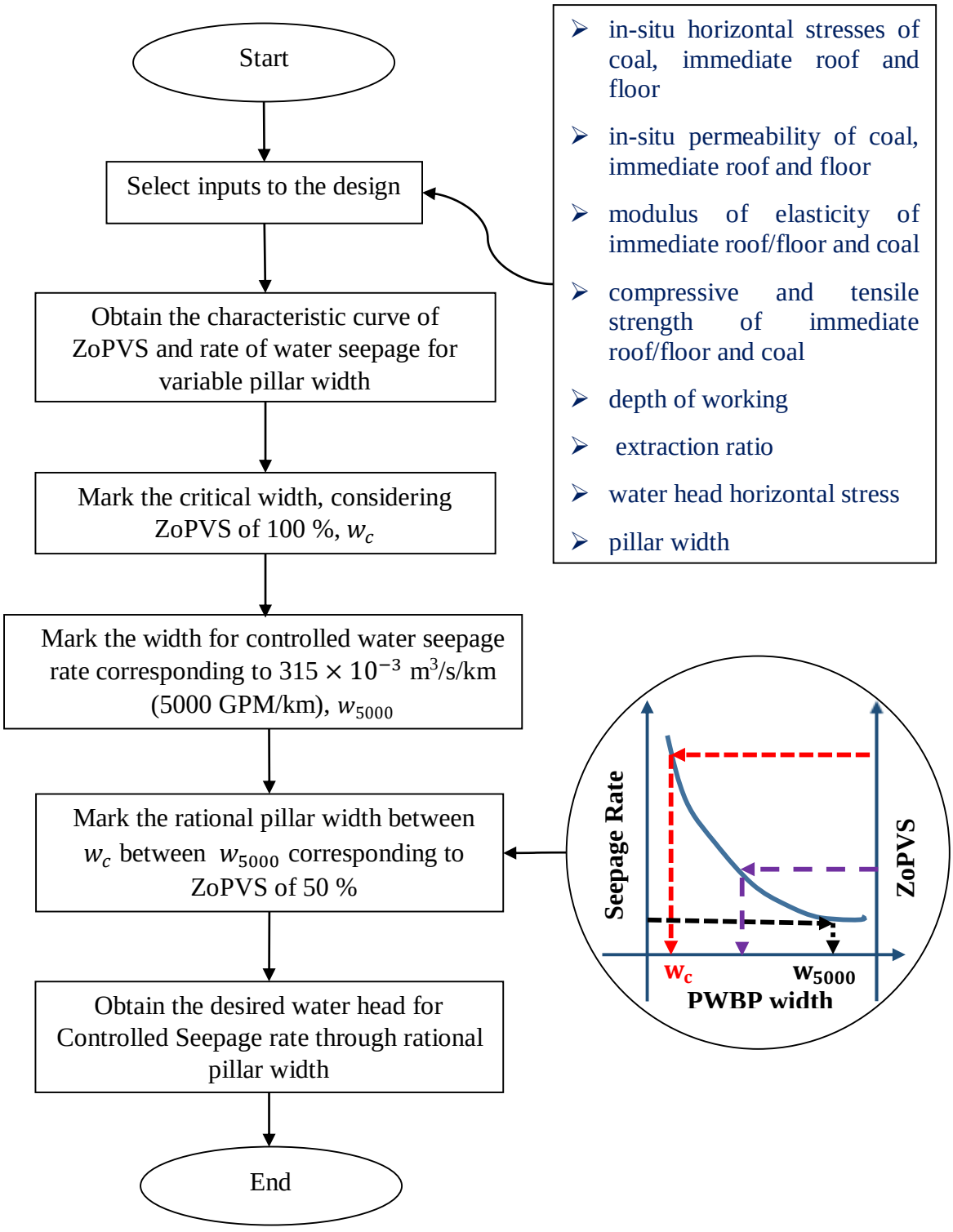

Figure 6.11. Flow chart illustrating the design of PWBP

6.8 Suggested Approach for Adequacy of the Existing PWBP

The flow chart shown in Figure 6.12 depicts the suggested approach for evaluating the adequacy of an existing PWBP for its long-term acceptable hydro-mechanical performance in a given geo-mining condition. It requires site-specific data on cover depth, extraction ratio, worst expected water head, H_w along with pertinent geo-mechanical properties of the coal seam and the immediate roof in terms of the modulus ratio of immediate roof/floor and coal pillar, the compressive strength of the coal, the ratio of the mean compressive strength and tensile strength of the pillar system as contained in Equation 6.4.

Step 1: The authenticated joint plan of the mine site is reviewed to evaluate the minimum width, w_m of the barrier along with the prevailing and the worst possible water head. If the same is not proven, the mine will take requisite steps to get the same established using geophysical or any other suitable method.

Step 2: The ZoPVS for the given minimum width of the barrier pillar is assessed to examine if it satisfies the criteria of critical pillar width for piping failure ZoPVS equal to 100 % confirms the potential for piping failure of the pillar that may cause inadvertent inundation in the active mine working.

Step 3: If the ZoPVS is less than the critical limit of 100 %, the seepage rate for the prevailing width of the barrier pillar is assessed.

Step 4: The severity of seepage rate is assessed by comparing the estimated seepage rate with the limits mentioned in the Severity classification table (Table 6.1). If the severity of seepage rate is 'Class III', the pillar size is considered inadequate. Otherwise, it is adequate for the given water head.

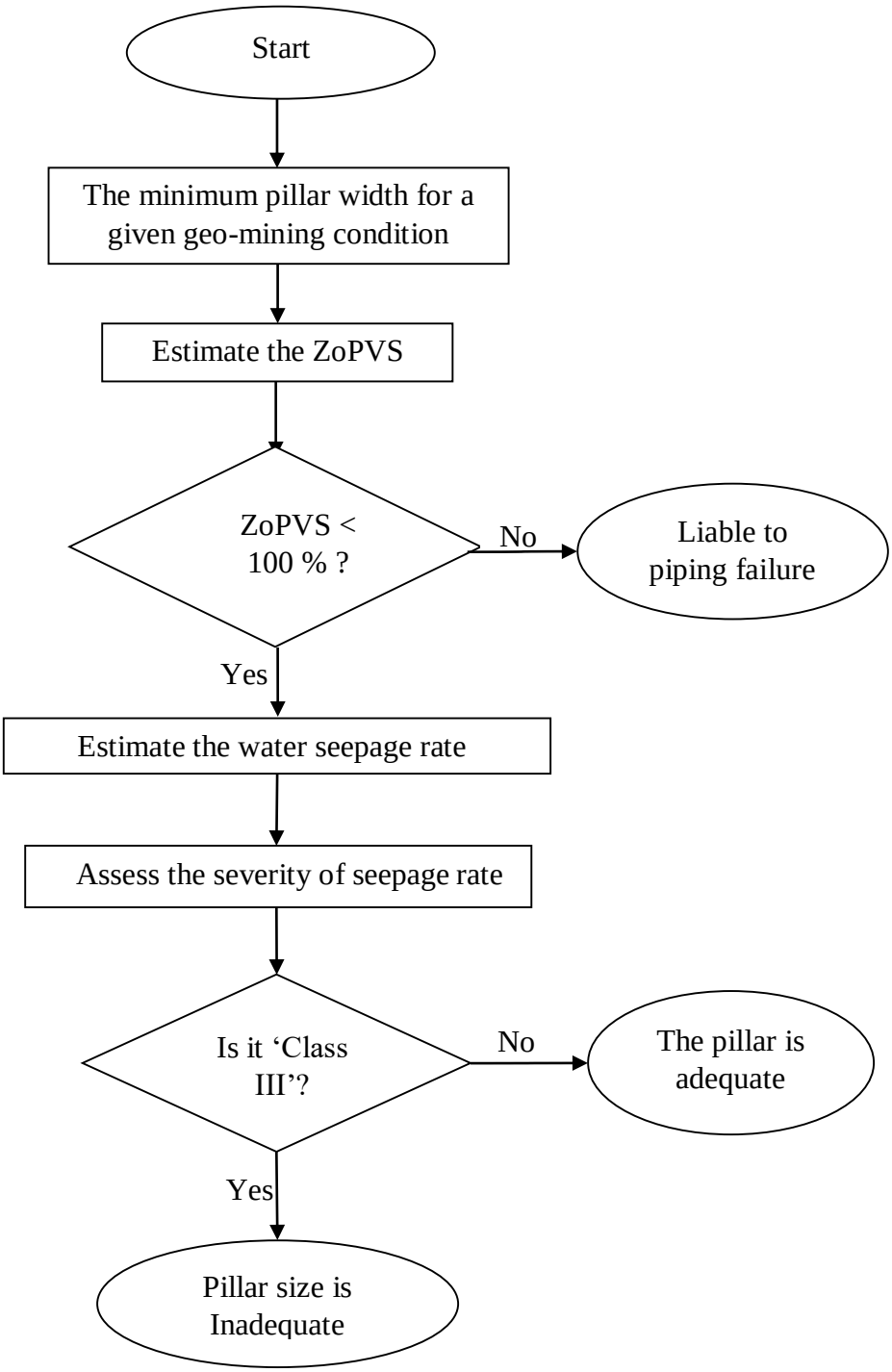

Figure 6.12. Suggested approach for assessment of the adequacy of existing PWBP

6.9 Summary

A set of governing relations were established for predicting the extent of ZoPVS and the seepage rate through the barrier pillars in different conditions. The ZoPVS had a positive correlation with the ratio of modulus of elasticity of roof/floor and coal, cover depth, and extraction ratio, but it was negatively correlated with the mean horizontal stress, compressive strength of coal, and pillar width. The seepage rate showed a positive correlation with the permeability, cover depth, water head, modulus, strength, and extraction ratios. However, it was negatively correlated with in-situ horizontal stress and pillar width. These relations have very high statistical significance and can be used for predicting the hydro-mechanical performance of PWBP in any geo-mining condition. The ZoPVS represented the extent of mechanical failure in the pillar, while the seepage rate was used as a parameter for assessing its hydraulic performance.

A seepage rate severity classification was proposed combining the numerical modelling outcome for the pillar system and the prevailing practice pertaining to pumping operation in the mine. It considered the rate of seepage required for knee-depth ponding up to a two-pillar distance within the standby time of 10 hours per day to evaluate the class of severity of seepage rate through the PWBP. Seepage rate greater than 315×10^{-3} $m^3/s/km$ (5000 GPM/km) marked 'Class III' severity, while less than 95×10^{-3} $m^3/s/km$ (1500 GPM/km) seepage rate marked 'Class I' severity.

The characteristic curves for ZoPVS and the rate of water seepage were obtained in soft and hard rock conditions at the water head of 25-100 % of the cover depth of 100-350 m. The 'critical width' liable to undergo piping failure corresponding to 100 % of ZoPVS, the 'controlled seepage rate width' corresponding to the seepage rate of 315×10^{-3} $m^3/s/km$

(5000 GPM/km), and the ‘rational pillar width’ indicated by ZoPVS of 50 % were identified for the worst water heads in different conditions. The standard approach for the rational design of PWBP and evaluating the efficacy of existing PWBP were also suggested.